Characterization by CO/FTIR spectroscopy of Pd/silica catalysts and its correlation with syn-gas conversion

Griselda C. Cabilla, Adrián L. Bonivardi and Miguel A. Baltanás *

INTEC (Instituto de Desarrollo Tecnológico para la Industria Química, Universidad Nacional del Litoral and Consejo Nacional de Investigaciones Científicas y Técnicas), Guemes 3450, 3000 Santa Fe, Argentina
E-mail: tderliq@arcride.edu.ar

Received 4 June 1998; accepted 14 September 1998

Well-dispersed Pd catalysts, supported on two morphologically different silicas (meso- and microporous Davison G59 and G03 grades, respectively) and used for syn-gas activation at $T = 493$–523 K and $P = 1$–4 MPa ($CO/H_2 = 1/2.5$), have been studied by CO chemisorption using FTIR spectroscopy. The long-term exposure to 760 Torr CO(g) at 298 K produces deep changes on the surface structure of Pd particles on both supports. The Pd particles become rougher and/or show more open crystal planes. This phenomenon of surface restructuring seems to depend both on the exposed metal fraction (FE) of palladium and the morphology of the support. The rate of surface restructuring but not its extent, is a function of the superimposed CO(g) pressure. On the microporous G03 silica CO chemisorbs in multicoordinated or "hollow" sites (H band), but these signals are not shown by preparations of the supported metal of comparable dispersity on mesoporous G59 grade. Terminal (L band) and di-coordinated CO_s (B band) appear in both types of catalysts. The high-loading preparations on the microporous support showed a higher proportion of Pd(111) planes than those of low Pd loading, which seems to contribute to the high TOF_{CH_4} and high selectivity to methane in syn-gas activation of these catalysts, while the remaining ones show excellent capability for methanol production.

Keywords: syn-gas conversion, FTIR spectroscopy, supported palladium, surface restructuring

1. Introduction

Poutsma et al. first demonstrated that the hydrogenation of carbon monoxide over silica-supported palladium could give methanol in high selectivity over a wide range of temperature and pressure conditions [1]. However, subsequent work by other research groups also showed that the activity and selectivity of Pd/SiO_2 for syn-gas conversion depend in a complex fashion on metal dispersion, crystallite morphology and support structure [2–4]. It is widely accepted now that the combination of the catalytic properties of a transition metal with the steric constraints imposed by a given support structure carries great potential for obtaining unique active and selective catalysts [5].

In a previous work by some of us, we used two structurally different, chemically purified silicas (meso- and microporous Davison G59 and G03 types, respectively). Reaction tests at $T = 493$–523 K and $P = 1$–4 MPa ($CO/H_2 = 1/2.5$) followed a careful follow-up of each of the preparation steps leading to the final catalysts [6]. Methanol was the main product on the mesoporous silica but on G03 methane selectivity was prevalent. Moreover, selectivity patterns were found to be very dependent on metal loading *only* on the microporous silica. On both support types the TOF_{CH_3OH} decreased smoothly, but TOF_{CH_4} showed a marked descent, by increasing the exposed metal fraction (FE) of palladium. Also, under pseudo-steady-state conditions ($t_R > 20$ h) the reactivity to methane was almost ten-fold higher on G03 than on G59 whereas the TOF_{CH_3OH} was about equal. Traces of ethane were found only on the former catalysts [6].

The use of CO as a surface probe, able to help in identifying the surface morphology of metal crystallites via FTIR spectroscopy has been repeatedly put forth in the last decades ([5,7,8] and references therein). On palladium single-crystal surfaces the vibrations of chemisorbed CO have characteristic frequency values for each of the exposed planes [8]; silica-supported Pd shows quite similar CO frequencies [9].

During a detailed CO/FTIR study aimed at elucidating the role of the support in promoting methanol synthesis over Pd/SiO_2 and Pd/La_2O_3, while purposedly trying to differentiate the effects of Pd dispersion and crystallite morphology from the effects of metal–support interactions, Hicks and Bell showed that the Pd morphology, as expressed by the distribution of Pd(100) and Pd(111) planes, could greatly influence the specific activity and selectivity for methanol synthesis: Pd(100) was nearly three-fold more active than Pd(111). For a fixed morphology, though, the specific methanol synthesis activity of Pd/La_2O_3 was a factor of 7.5 larger than that of Pd/SiO_2 [7].

Many other workers have paid attention to the impact of other features of the morphology of metal crystallites on the reactivity. For example, it is well known that the sticking coefficient of gaseous adsorbates can increase substantially owing to the presence of particle surface defects [10]. Also, Somorjai and co-workers have extensively shown that dif-

* To whom correspondence should be addressed.

ferent amounts of corners, edges, kinks and steps can deeply affect the reactivity of adsorbed hydrocarbons (hence, the reaction selectivity) owing to the different C–C and C–H bond breaking properties of those surface sites [11–13].

However, Somorjai and van Hove have demonstrated that the chemisorption of atoms or molecules which may form strong metal–adsorbate bonds (e.g., O_2/Al(110), CO/W(111), O/Cu(100), S/Ir(110), etc.) usually induces reconstruction of the metal surface. They pioneered the concept that "the act of adsorption gives rise to a dynamic change of surface structure, often reversible, sometimes permanent" [14]. El-Yakhloufi and Gillet [15] deposited Pd particles onto saffire single crystals, using SSIMS to study CO chemisorption at 300 K under UHV conditions. They found that CO could reconstruct the Pd surface, increasing the Pd–Pd distances, above 0.2 of saturation coverage. More recently, Hicks et al. reported that cycles of CO exposure and reduction of Pd/Al_2O_3 at ambient pressure (<200 Torr) smooth the crystallite surfaces into well-ordered facets, whereas cycles of oxidation and reduction roughen the surfaces [16].

This led us to re-examine our Pd/SiO_2 catalysts, using CO/FTIR spectroscopy, to conduct *in situ* studies about a possible surface restructuring of the palladium crystallites supported on these two chemically equivalent but structurally different (meso- and microporous) silicas [17] and to correlate these data with their dissimilar activity and selectivity performances in syn-gas activation. Long-term exposures to CO(g) at 10 and 760 Torr were used throughout this work.

2. Experimental

2.1. Materials

Catalytic materials were obtained via ion exchange (IE) of $[Pd(NH_3)_4]^{2+}$, prepared from 99.5% w/w palladium acetate (Engelhard Corp.) on two commercial gels of silica (Davison G59: $S_g = 254$ m^2/g, modal radius = 83 Å, and Davison G03: $S_g = 558$ m^2/g, modal radius = 16 Å). Ion exchanges were made under standardized conditions, at pH = 11 and 298 K ("room temperature", RT), in aqueous alkaline solution. After washing at same pH, the catalysts were dried in air at RT during 24 h. Support characterization and IE procedures have been fully detailed in previous work [17].

The catalyst precursors were calcined in air from RT to $T_c = 623$ K with a heating rate, β, of 6 K/min, then held at T_c for 2 h and cooled back to RT under gas flow. Next, they were reduced in hydrogen from RT to $T_r = 723$ K ($\beta = 2$ K/min), held at T_r for 2 h and cooled back to RT under gas flow. The percent exposed metal fractions (FE) of these materials were determined by using H_2 chemisorption at 298 K and controlled with XRD and TEM [18,19].

Palladium loadings were selected to obtain either low ($\theta = 0.2$) or high ($\theta = 0.6$–0.7) metal surface coverages.

Table 1
Characteristics and codes of the catalysts.

Support[a]	Pd loading[b] (% Pd w/w)	Pd surface coverage[c] (θ)	FE[d] (%)	$\bar{d}_p$[e] (Å)	Catalyst code
G59	1.1	0.18	76	15	Pd/G59-L76
	3.7	0.62	56	20	Pd/G59-H56
G03	2.2	0.20	65	17	Pd/G03-L65
	7.7	0.72	77	14	Pd/G03-H77
	7.7	0.72	53	21	Pd/G03-H53

[a] Davison silica, mesoporous (G59) and microporous (G03) grades.
[b] After ion exchange of tetramminepalladium acetate in aqueous alkaline solution ($R = 30$ ml solution/g support, pH = 11, $T = 297$ K), then washed at pH 11, then air dried at 298 K during 24 h in a forced convection oven.
[c] $\theta = \Gamma_i/\Gamma_s$, Γ_i = mmol Pd/m^2, Γ_s = saturation value [17].
[d] Initial exposed metal fraction. Chemisorption stoichiometry: $H_{ad}/Pd_s = 1$ [19].
[e] Average metal particle diameter, $d_p = 1.12/FE$ [19].

Henceforth, the catalysts are coded with either L or H labels, followed by their initial FE, for a straightforward follow-up (see table 1).

Gas sources were: N_2 99.999% (Scott U.P.G.), H_2 99.999% (Scott U.P.G.), He 99.9999% (Matheson purity) and CO 99.999% (AGA, Research Grade). All the gases were purified to remove O_2 and water with 3 Å molecular sieve (Fisher Co.) and MnO/Al_2O_3 cartridges. A granulated ascarite (Thomas Scientific pro-analysis) cartridge was also added to the CO line to remove CO_2.

2.2. Experimental procedures

Pellets of 10 mg/cm^2 of each catalyst were prepared by pressing at 5 ton/cm^2 (Pd/G59 samples) or 7 ton/cm^2 (Pd/G03 samples). All catalyst pretreatments and measurements were performed *in situ* in a flow-type Pyrex infrared cell (NaCl windows) attached to a high-vacuum system (base pressure = 10^{-6} Torr), furnished with programmable heating and window cooling devices. The cell was mounted into the sample chamber of a Shimadzu model 8100 single-beam FTIR spectrometer equipped with a narrow-band HgCdTe detector. The chamber was continuously purged with dry air. All spectra were collected at 4 cm^{-1} resolution. Generally, 100 scans were used for each spectrum to obtain satisfactory signal to noise ratios, with each spectrum taking about 160 s. Blank experiments confirmed the absence of significant CO adsorption on the metal-free silicas.

Each catalyst pellet was reduced *in situ* under flowing H_2 (100 cm^3/min) at 523 K during 1 h ($\beta = 2$ K/min) after purging the cell with nitrogen at RT for 15 min. Adsorbed hydrogen on Pd was eliminated by evacuating the cell at 653 K for 2 h ($\beta = 10$ K/min). The sample was subsequently cooled down to RT. Background IR spectra of these "clean" samples were obtained at each temperature for their further subtraction from adsorbed CO spectra.

A sequence of IR spectra of adsorbed carbon monoxide (CO_s) was then recorded, according to the following proce-

dure: The sample was exposed to 10 Torr of pure CO(g) at RT and a spectrum was immediately taken ($t^{\mathrm{I}} = 0$ h). Then, the cell pressure was increased to 760 Torr and it was kept constant until the next spectrum was recorded. Next, each following CO_s spectrum was taken, after a fast evacuation of the cell to 10 Torr *only* during the spectrum acquisition time, to reduce background noise correction. Soon afterwards, the pressure in the cell was again reestablished to 760 Torr CO(g); this procedure took less than 5 min each time.

The last adsorption spectrum was taken after a total exposure of about 18 h at 760 Torr, after which CO was removed by evacuating and then heating the sample under vacuum up to 653 K ($\beta = 3$ K/min). Next, the cell was cooled down again (*in vacuo*) to RT, after which a new dose of 10 Torr CO(g) was admitted into the cell and a final IR spectrum was recorded ($t^{\mathrm{II}} = 0$ h).

An additional experiment was conducted, to study the possible impact of a lower CO(g) pressure on crystallite restructuring, by exposing a fresh sample of Pd/G59-L76 just to 10 Torr CO(g), for 1 h, while taking spectra every 10 min.

The IR spectra were processed as follows: background spectra of the clean samples (obtained at each temperature) were subtracted. Further subtractions were also made to remove the gas-phase interference from the bands due to chemisorbed CO. Background noise correction and Gaussian deconvolution of chemisorbed CO bands were done on digitalized spectra, by means of a commercial software (Microcal Origin® 4.1 w/Peak Fitting Module).

3. Results and discussion

3.1. CO adsorption

Infrared spectra of CO_s (CO(g) = 10 Torr) adsorbed at RT on Pd/G59 and Pd/G03 catalysts taken at $t^{\mathrm{I}} = 0$ h are shown in figure 1. In general, two well-reported types of chemisorbed carbon monoxide on palladium are identified in these CO/FTIR spectra [7,8,20]. The band close to 2095 cm^{-1} is attributed to terminal, monocoordinate or linearly bonded CO (L). Broad, convoluted bands appear under 2000 cm^{-1}; they are assigned to multicoordinated, bridging CO: B_1, corresponding to di-coordinated, bridging CO on structurally open crystal planes, e.g., (100) or (210), close to 1970 cm^{-1}; B_2, corresponding to di-coordinated, bridging CO on Pd(111), around 1956 cm^{-1}, and a band below 1830 cm^{-1} (herein, H band), usually assigned to triply bridging CO on Pd(111) "hollow" sites. Band assignment of chemisorbed CO on supported palladium is straightforward, since these bands locate at slightly lower frequencies (15–20 cm^{-1}) than on Pd single crystals [7,8,21].

It is immediate that both the L and B bands are noticeably present in each of the catalysts. However, the relative intensity of these bands varies amongst them; L/B is largest for the highly dispersed palladium on mesoporous silica sample (Pd/G59-L76). Indeed, this feature is to be expected when changing the Pd particle size and it has been extensively reported over suported palladium catalysts [7,22,23].

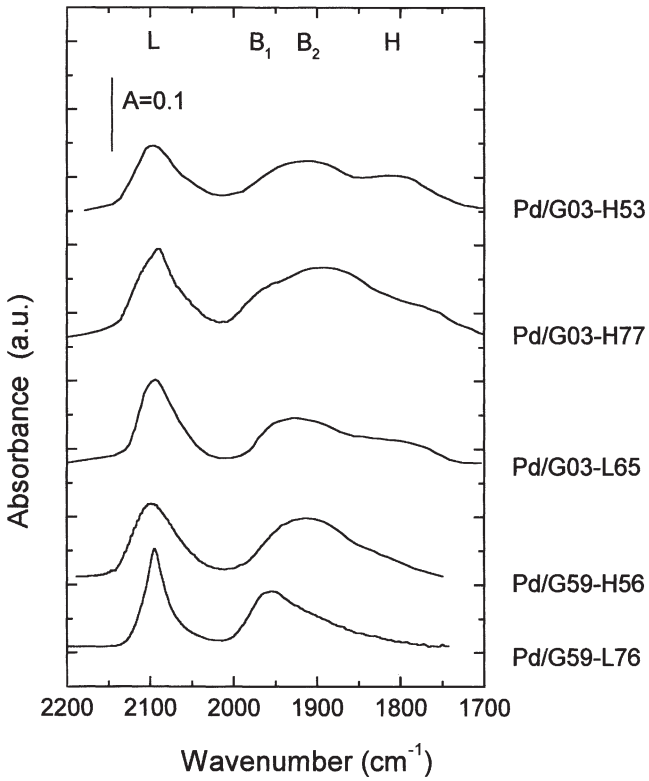

Figure 1. FTIR spectra of CO (10 Torr) adsorbed at 298 K (RT) on the Pd/G59 (mesoporous) and Pd/G03 (microporous) silica catalysts ($t^{\mathrm{I}} =$ 0 h). Samples were pre-reduced *in situ* under flowing H_2 (100 cm^3/min) at 523 K during 1 h ($\beta = 2$ K/min), then evacuated at 653 K for 2 h ($\beta = 10$ K/min) and cooled down to RT.

A similar behavior is observed for the relative intensity of the B_2 and B_1 bands: the B_2/B_1 ratio is the larger the lower the metal dispersion is. As was suggested by Bell and co-workers [7] the distribution of the Pd(111) and Pd(100) surface planes can be obtained from this intensity ratio, which is in agreement with a change in the metal particle size: the bigger the fcc cube–octahedron metal crystallites, the bigger the ratio of Pd(111) to Pd(100) plane [23].

The CO_s band on hollow (H) sites only appears on Pd supported on the microporous G03 silica. This agrees well with former results by Sachtler et al., who studied CO chemisorption, at total coverage, on palladium supported on NaY zeolites [24]. These workers found that after mild H_2 reduction and exposure to a flow of CO (1 atm) for 10 min at RT, with subsequent purging with Ar, a triply coordinated CO signal was apparent (1829 cm^{-1}). On extended surface domains, though, hollow-sites type CO adsorption has only been reported at very low coverages ($\theta < 0.1$ [8]). In our case, the H band on the Pd/G03 samples is also accompanied by an intense B_2 band, which becomes more intense the higher the Pd loading is (figure 1 and tables 2 and 3).

Table 2
Integrated areas of the CO/FTIR bands, corresponding to linear (L) and di-coordinated (B) carbon monoxide, on the Pd/G59 catalyst samples.

Exposure time (h)	Pd/G59-L76				Pd/G59-H56			
	Σ^a	Percentage of the absorbance area			Σ^a	Percentage of the absorbance area		
		L	B_1	B_2		L	B_1	B_2
0	1.00	38.9	14.9	46.2	1.00	38.1	0.9	60.9
0.5	1.17	37.6	21.7	40.9	1.88	37.4	1.6	61.0
1	1.14	37.7	21.3	41.0	2.00	38.2	2.0	59.6
1.5	1.14	37.0	31.4	41.6	1.94	40.0	3.7	56.2
2.5	1.19	35.4	21.0	43.6	2.18	37.8	3.9	58.2
3.5	1.18	34.7	22.0	43.2	2.08	39.7	3.7	56.7
18	1.22	35.0	20.5	44.4	2.05	42.2	5.1	52.7

[a] Σ stands for the ratio of total absorbance area, relative to the one measured at $t^{\mathrm{I}} = 0$ h.

Table 3
Integrated areas of the CO/FTIR bands, corresponding to linear (L), di-coordinated (B) and multi-coordinated (H) carbon monoxide, on the Pd/G03 catalyst samples.

Expos. time (h)	Pd/G03-L65					Pd/G03-H77					Pd/G03-H53				
	Σ^a	Percentage of the absorbance area				Σ^a	Percentage of the absorbance area				Σ^a	Percentage of the absorbance area			
		L	B_1	B_2	H		L	B_1	B_2	H		L	B_1	B_2	H
0	1.00	39.4	3.4	35.4	21.8	1.00	31.5	4.7	39.2	24.7	1.00	38.2	9.7	43.6	8.5
0.5	2.06	38.7	12.3	26.5	22.4	1.62	33.5	2.2	37.1	27.2	1.45	37.4	2.2	42.2	18.2
1	2.06	40.2	11.6	28.3	19.9	1.73	33.8	2.0	37.8	26.3	1.58	37.2	2.5	43.6	19.8
1.5	2.21	39.6	10.5	29.0	20.9	1.67	34.4	2.4	39.2	24.0	1.71	39.9	2.8	41.0	16.3
2	2.04	40.9	10.6	30.2	18.4	1.71	34.7	2.7	38.9	23.7	1.90	40.3	2.6	40.7	16.3
2.5	2.10	40.3	12.3	28.3	19.0	1.68	34.6	2.6	40.1	22.8	1.97	41.1	3.4	38.5	17.0
3	–	–	–	–	–	1.66	34.8	2.5	39.3	23.4	2.19	39.3	3.6	38.2	18.8

[a] Σ stands for the ratio of total absorbance area, relative to the one measured at $t^{\mathrm{I}} = 0$ h.

Table 4
Initial catalytic activities of the catalysts at 523 K, 3 MPa and $H_2/CO = 2.5$, expressed as TOF_i (mol_i ($i = CH_4$ or CH_3OH) s^{-1} Pd_s^{-1}).

$TOF_i \times 10^4$	Pd/G59-L76	Pd/G59-H56	Pd/G03-L65	Pd/G03-H77	Pd/G03-H53
TOF_{CH_4}	0.5	3	2	7.5	9
TOF_{CH_3OH}	14.5	22.5	5.2	5	4.2

Both features indicate that a larger proportion of Pd(111) planes exist [7,8] in the Pd crystallites deposited onto the G03 silica. So, it is worth emphasizing that the microporous silica is able to host highly dispersed Pd particles where multicoordinated CO adsorption sites, with weakened C–O bond energy, are favored.

Table 4 presents initial reactivity data for syn-gas activation on these catalysts at 523 K and 3 MPa, expressed as TOF_{CH_3OH} and TOF_{CH_4} based on the initial FE of the supported metal [6,25]. These values show that both Pd/G03-H53 and Pd/G03-H77 are highly selective to methane, while the TOF_{CH_4} of the low-loading Pd sample on the microporous silica is quite close to the ones on the mesoporous G59. The initial turnover frequency to methanol is higher on the latter catalysts, although at pseudo-steady-state conditions it became quite similar in the whole set of preparations [2]. The correlation between CO/FTIR patterns at $t^{\mathrm{I}} = 0$ h and initial reactivity data is clearly indicative of the microporous silica being able to host metal crystallites where multicoordinated CO adsorption sites, with weakened C–O bond energy – and thus able to dissociate – are favored.

The effect of prolonged exposure to 760 Torr CO(g) at RT on the metal particles morphology can be observed in figure 2. This figure compares the spectra of CO_s ($CO(g) =$ 10 Torr) after 3 h exposure on the Pd/SiO_2 catalysts to atmospheric carbon monoxide vs. the ones taken at $t^{\mathrm{I}} = 0$ h. Additional exposure up to 18 h did not modify these spectra any further.

It is apparent that the total amount of adsorbed CO on Pd, which is equivalent to the integrated area under the absorbance curve, increased with time in every case. However, these changes were not the same for each sample. This is indicated with detail in tables 2 and 3, which contain the ratios of the measured values of total absorbance vs. time, relative to the ones at $t^{\mathrm{I}} = 0$ h (Σ), as well as the percentage of the total absorbance corresponding to the L, B_1, B_2 and H bands, respectively.

Supplementary information can be obtained from figures 3 and 4, which show difference spectra at increasing

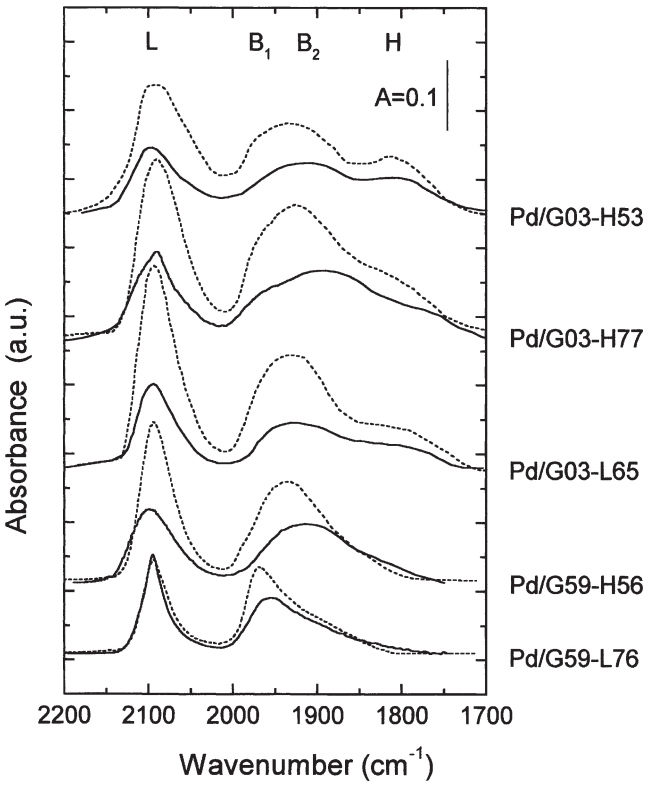

Figure 2. Comparative spectra of adsorbed CO (taken at 10 Torr; RT) on the Pd/SiO_2 catalysts after their exposure to 760 Torr CO(g) at the same temperature during: $t^I = 0$ h (initial exposure; continuous lines) and $t^I = 3$ h (dashed lines). Additional exposure up to 18 h did not modify these spectra any further.

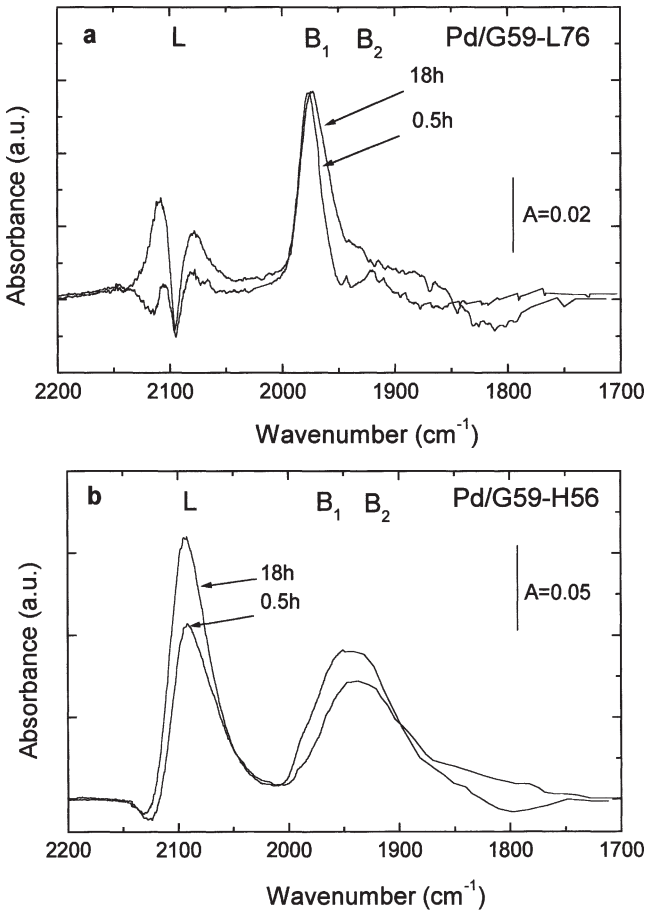

Figure 3. Difference spectra of adsorbed CO (taken at 10 Torr; RT) on the Pd/G59 catalysts after their exposure to 760 Torr CO(g) at the same temperature at increasing times of exposure, subtracted from the CO_s spectra taken at $t^I = 0$ h.

time of exposure, subtracted from the CO_s spectra on the Pd/G59 and Pd/G03 samples taken at $t^I = 0$ h, respectively. This representation allows one to focus the attention only on the *changes* experienced by the various adsorbance bands after each time interval during which the materials were exposed to CO at 760 Torr. The absence of any shifts in the band positions are proper of full CO_s coverage spectra in every case [9].

Spectra in figure 3(b) indicate that the band intensities of both terminal and multi-coordinated CO_s increased when the larger metal crystallites of Pd on the mesoporous silica (Pd/G59-H56, $d_p = 21$ Å) were exposed to CO. Likewise, each of the CO_s bands grew on the microporous silica preparations, regardless of the particle size or metal loading (figure 4); the increase in total absorbance was superior to 100% on Pd/G59-H56 and Pd/G03-L65, and above 75% on Pd/G03-H77 and Pd/G03-H53. For the highly dispersed palladium particles on the mesoporous G59 (Pd/G59-L76, $d_p = 14$ Å), in contrast, only the B_1 band showed a significant growth (figure 3(a)).

These increases in total absorbance are not due to diffusional "problems" or to activated adsorption kinetics. Every calculation of characteristic diffusion times using data of the support structures (mean pore radii and tortuosity) for a 100 μm pellet thickness and the Bosanquet equation for the diffusion coefficient [26,27] gave us just less than a one-hundredth second for the CO(g) to reach the pellets center. As for the adsorption kinetics, Chou and Vannice [28] have shown, using calorimetric heat of adsorption measurements, that CO chemisorption rapidly proceeds on Pd: the energy changes due to adsorption after the introduction of 75 Torr CO(g) to the DSC chamber at 300 K were complete in less than 2 min. Also, Eley and Moore [29] have reported that total CO coverage of Pd is reached after exposures to just 5 L (1 L $= 10^{-6}$ Torr s). Therefore, the up to two-fold growth in the CO_s band intensities after the long-term exposure to the gas has to be attributed to a surface reconstruction, which increases the exposed metal surface area.

Additional information is provided by figure 5, which shows the area ratios of the L and (B + H) bands (measured at 10 Torr CO(g)), as a function of the time of exposure to CO(g) at 760 Torr. This L/(B + H) ratio increases with increasing exposure time for Pd/G03-H77, Pd/G03-L65 and Pd/G59-H56, and again strongly suggests that the Pd crystallites become rougher upon long-term exposure to the gas. In previous paragraphs we have assigned the L band to terminal CO, linearly bonded to planes, edges and corners on the Pd surface [30], whose proportions vary with particle size and/or morphology changes [23].

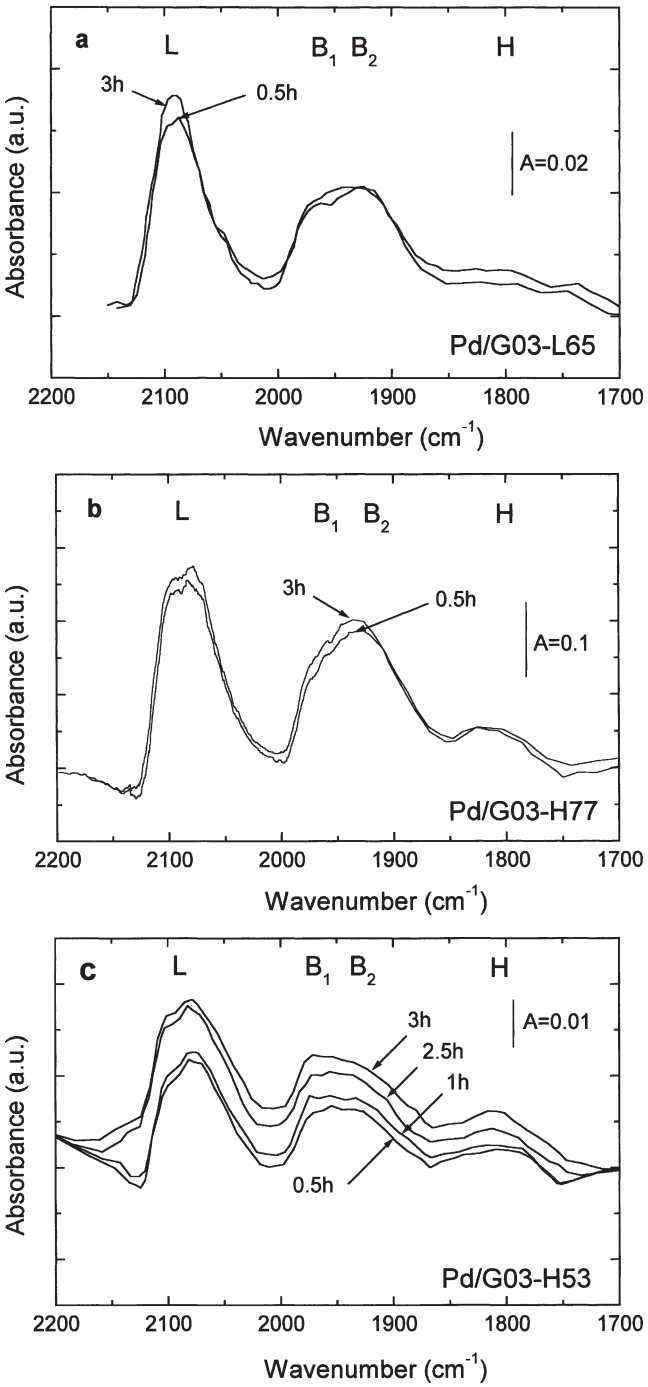

Figure 4. Difference spectra of adsorbed CO (taken at 10 Torr; RT) on the Pd/G03 catalysts after their exposure to 760 Torr CO(g) at increasing times of exposure, subtracted from the CO_s spectra taken at $t^I = 0$ h.

Bradshaw and Hoffmann have shown that the π-character of the M–CO bond is lower when the coordination number is smaller. Their data suggest that back-donation from the metal to the ligand is highest for Pd atoms in terraces of Pd crystal surfaces. Isolated or protruding atoms (e.g., in corner or edge positions or in "open" crystal faces) appear to be less efficient electron donors [31]. The conclusion that linear CO is preferentially formed on low-coordinated Pd atoms immediately implies that the L/B ratio should

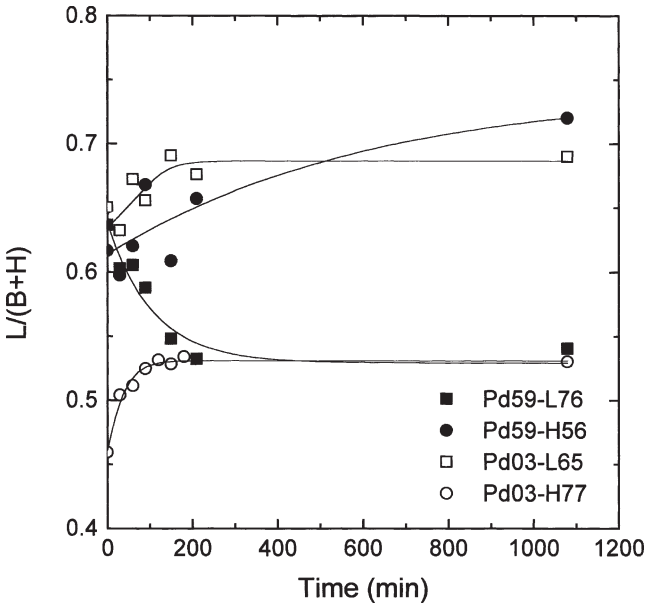

Figure 5. Relative intensity (area ratio) of the terminal (L) and "bridging" (B + H) CO_s bands (measured at 10 Torr CO(g) and RT) on the Pd/SiO_2 catalysts, as a function of the time of exposure to 760 Torr CO(g).

increase with *decreasing* particle size, because smaller particles expose a larger fraction of low-coordinated (corner or edge) atoms than larger particles, if all other factors are kept equal. On the same grounds, though, progressively rougher particles should also show increased L/B band intensity ratios.

The behavior of the Pd/G03-H53 sample, with a steady increase in total absorbance and no definite L/(B+H) trend, is atypical (see figure 4(c) and table 3). This may be due to a partial occlusion of the metal particles owing to the high loading of the metal on the microporous support [19]. The total absorbance of these bands is indeed very low ($A \approx 0.06$ for the strongest band at 1970 cm^{-1}).

As regards the highly dispersed palladium catalyst supported on the mesoporous silica (Pd/G59-L76, $d_p = 14$ Å), only the B_1 bands intensity increased with time of exposure to CO (figure 3(a)). Thence, the L/(B + H) area ratio decreases with exposure time, as illustrated in figure 5. The reason why only the bridge-bonded CO_s intensity changes is difficult to recognize. As the total absorbance increased in about 25% with time, one is forced to disregard an invocation to particle growth, coalescence or loss of dispersion of the Pd particles. Another plausible explanation is to think of a local surface reconstruction of the metal planes without an increase in the amount of low-coordination sites, which are mainly responsible of adsorbed linear CO.

In this respect, it is noteworthy to recall that Bradshaw and Hoffmann [31] have shown that the behavior of the di-coordinated CO_s band on the very open Pd(210) surface resembles that of the Pd(100) surface. Two differences between these surfaces are that the IR frequency of the two-fold coordinated CO locates on Pd(210) at about $+50$ cm^{-1} with respect to its position on the Pd(100) surface, and that no L band is observable, even at full CO_s

coverage, on the former plane. Also, these authors proposed a surface model of (1×2) structure for adsorbed CO on Pd(210) that implies a stoichiometry of CO to the outermost layer of the Pd atoms equal to $3/2$, because metal atoms of the second and third layers might also be involved in direct bonding to CO [31,32]. A closer analysis of the B_1 band on the spectra of the Pd/G59-H76 sample (see figures 2 and 3(a)) shows that indeed its position shifted to higher frequencies, from 1960 to 1978 cm^{-1}, with CO exposure time. Although we cannot confirm the presence of the Pd(210) plane in our material, it seems logical to think of that, if the metal particles are small enough for the carbon monoxide to restructure them, making more open palladium surfaces.

An isolated look at the final L/(B + H) area ratios in figure 5 could lead to thinking, erroneously, that the CO/FTIR spectra of the Pd/G03-L65 and Pd/G59-H56 pair of catalysts, or the ones pertaining to the Pd/G03-H77 and Pd/G59-L76 pair, should be similar. Figure 3 shows that not being the case. In fact, the pronounced dissimilarities that characterize the CO_s spectra on both grades of silicas remain during the course of the experiments, regardless of the time of exposure to the gas, independently of the values adopted by the area ratios. Some authors have proposed using the ratio of linear to bridged CO_s as a good benchmark to estimate the dispersion of Pd on silica [20]. In view of our results we are inclined to recommend judicious use of that suggestion whenever structurally different silicas are employed.

The importance or not of the surface morphology of the metal crystallites on the catalyst performance of supported Pd to activate syn-gas selectively to methanol or to methane can be addressed now.

Two substantially different mechanisms have been proposed to explain the differences found using CO/H_2 on promoted Pd/silica. Ponec's group assigns a key role to positive palladium ions which are stabilized by MgO as promoter. They reported the existence of a direct correlation between the methanol activity and the amounts of extractable Pd^{n+} species leached from the catalysts under oxygen-free conditions [3]. Support to Ponec's view was provided by ESR observations of Cl-containing MgO promoted palladium [33]. Shen et al. proposed the hydrogenation of $Pd^{+}HC(O)OMg^{2+}$ intermediates as the rate-determining step to methanol formation [34]. However, Cl-free catalysts did not show any observable metallic cation in spite of their good methanol yields [35]. Furher studies by infrared spectroscopy have found no evidence between the existence of Pd ion sites on the surface and methanol production: a very weak band at 2165 cm^{-1} suggesting the adsorption of CO over a Pd^{n+} ion was observed by Deligliani et al. in one of their least active catalysts [36]. Nonetheless, special attention was paid in this work to detect possible adsorption of CO on palladium ions over our catalysts. Yet, no CO bands above 2100 cm^{-1} were ever observed over our unpromoted catalysts.

The other mechanism involves CO chemisorbed onto Pd^0 followed by reaction with hydrogen, to give CH_xO intermediates (like formate, formyl or hydroxymethylene) in methanol synthesis – where no dissociation of the C–O is involved – or, conversely, to methane. In the absence of any kind of promoter (chlorine and/or alkaline elements) one is tempted to look first at methane production in an effort to provide additional understanding or the catalytic performance of our silica-supported palladium catalysts. Vannice found an excellent correlation between the specific activity of transition metals in methane synthesis and the strength of the adsorbed CO–metal bond, determined by heats of adsorption. A kinetic model that assumes the rupture of the strong C–O bond (256 kcal/mol [37]) as the rate-determining step in this reaction was put forward [38]. In another study, Winograd et al. [39] found that thermally induced decomposition of CH_3OH on Pd(111) proceeds through a pathway which involves the formation of $(CH_3)_{ads}$. This intermediate was unusually stable (up to 400 K). Put it into other words, on Pd(111) the C–O bond is activated with relative ease. On the other hand, Solymosi et al. [40] have worked extensively on adsorption and decomposition of methanol on Pd(100) and found no evidence of activation of the C–O bond on this plane. They found, instead, that CH_3OH decomposition proceeds via adsorbed methoxy species; no $(CH_3)_{ads}$ nor water or methane in the products stream was found either. It is but logical, then, to associate the preponderant presence of the B_2 *and* H bands on the Pd/G03 catalysts to their superior methanation ability, as these low-frequency CO stretching bands correspond to a weakened C–O bond.

Further inspection of figure 5 reveals that the changes in the L/(B + H) area ratio on the Pd/G03 catalyst samples stop after 2 h exposure while those on the mesoporous G59 silica last much longer. These results could find a possible explanation if the microporous G03 silica would hamper further reconstruction and/or roughening of the Pd particles. Thus, the morphology of the support could be affecting the surface restructuring of the metal crystallites.

One extra experiment to test the effect of CO pressure over Pd/G59-H76 was done. In this case, the sample was continuously exposed to 10 Torr of CO(g) and IR spectra were taken after different time intervals at this pressure. The features of the B bands are shown in figure 6, which shows difference spectra at increasing time of exposure, subtracted from the CO_s spectra taken at $t^{I} = 0$ h. While the enlargement of the B bands increase is similar to the one at 760 Torr exposure, described above, the changes in intensity are slower at the lower pressure. Thus, surface restructuring of silica-supported Pd crystallites seems to be directly affected by CO(g) pressure: the higher the pressure, the faster the surface reconstructs.

3.2. CO desorption

As indicated in section 2, after their exposure to 760 Torr CO(g) for 18 h the samples were evacuated at RT for the

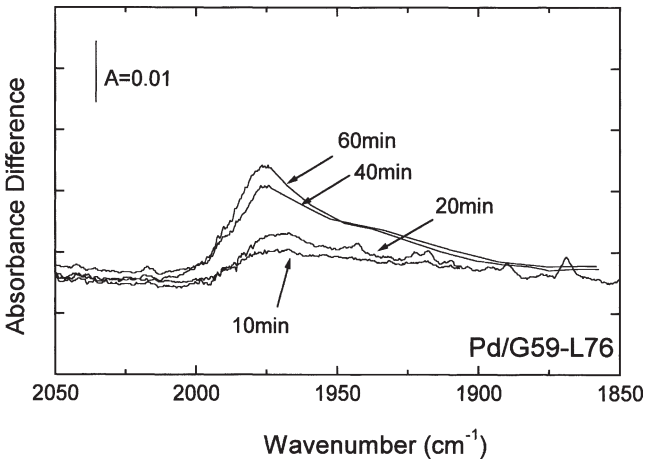

Figure 6. Difference spectra of adsorbed CO on the Pd/G59-L76 catalyst after its continuous exposure to 10 Torr CO(g), subtracted from the spectrum taken at $t^1 = 0$ h ($T = 298$ K).

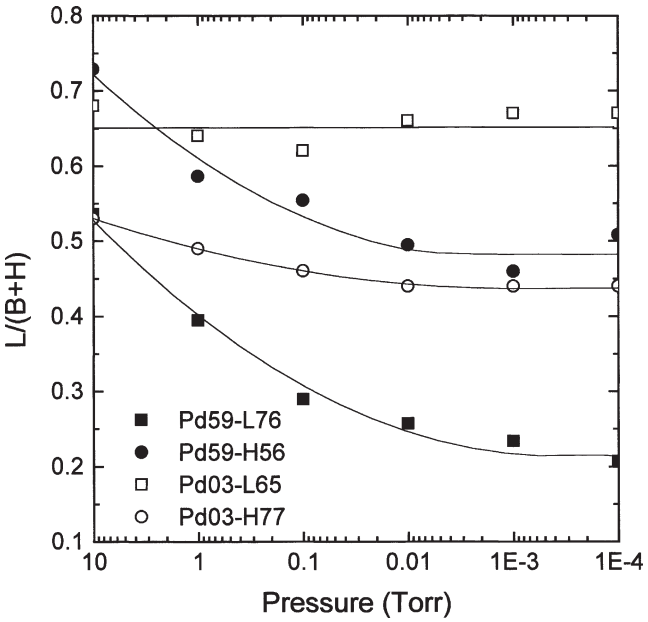

Figure 7. Relative intensity (area ratio) of the terminal (L) and "bridging" (B + H) CO_s bands on the Pd/SiO_2 catalysts, as a function of evacuation pressure ($T = 298$ K). Total evacuating time was 30 min.

same length of time (30 min), down to 5×10^{-4} Torr. During this procedure all gaseous and weakly bonded carbon monoxide leave the catalyst surface, together with a minor fraction of the chemisorbed CO. Carbon monoxide desorption at RT is slow; as the heat of adsorption of CO on Pd is known to be 30 kcal/mol [41] it follows that the activation energy for desorption must be equal or larger than this, and that thermal desorption at RT must be very slow.

Yet, the decrease in total absorbance was dissimilar on the two Pd/SiO_2 catalyst types: a 25% reduction was observed on the Pd/G59 samples (relative to the integrated areas corresponding to the restructured surfaces), whereas almost no reduction in total absorbance was observable on the catalysts supported on the microporous silica. The Pd/G59 samples showed the well-known desorption pattern

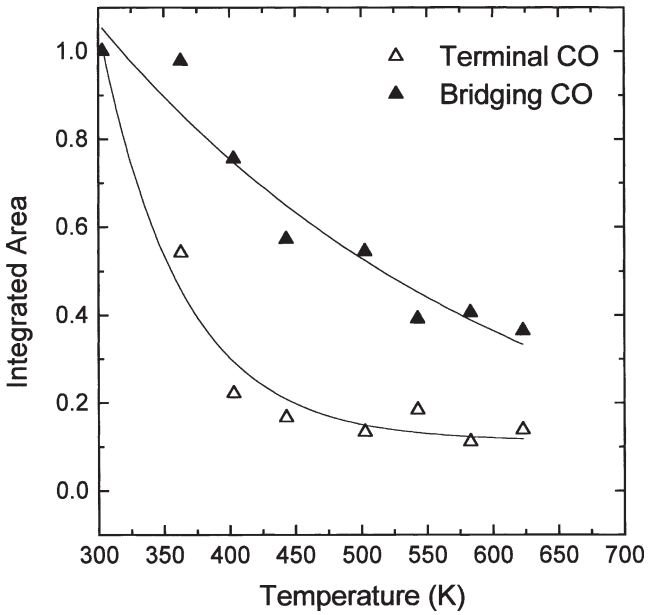

Figure 8. Integrated areas of the terminal and "bridging" CO_s bands on the Pd/G59-L76 catalyst, as a function of desorption temperature, relative to their intensity at 298 K and $P = 5 \times 10^{-4}$ Torr ($T_{max} = 653$ K).

at room temperature [5,7]: while the linearly bonded CO partially desorbed, the bridging and multicoordinated bands did not change noticeably. Consequently, the L/(B + H) ratios steadily fell on the mesoporous silica catalysts only (figure 7). It seems, then, that the use of static evacuation rather than, e.g., cell purging with an inert gas [24] is insufficient for CO_s removal at RT onto small metal particles deposited on a microporous support.

The samples were then subjected to temperature-programmed desorption ($\beta = 3$ K/min), *in vacuo*, up to 673 K, with constant FTIR monitoring. At this temperature most of the CO_s (about 75% of the total) was removed from the catalysts, as expected [42]. Each of the catalyst samples displayed the classical desorption sequence: terminal CO was almost completely desorbed at 453 K, but some multicoordinated carbon monoxide still remained (about 25% of the B + H bands), which agrees well with former observations of Bell and co-workers [7]. At higher temperatures, i.e., at lower surface coverages, the maxima of the B band shifted progressively to lower frequencies, as bridge-bonded CO_s on the Pd(100) planes is more weakly held than bridge-bonded CO on Pd(111) planes [9,43].

Figure 8 depicts typical (absorbance) peak areas vs. desorption temperature for the terminal and multiply coordinated CO_s, obtained for the Pd/G59-L76 sample. It is apparent that (a) adsorption energy for linear CO_s is much lower than for bridging CO, and (b) that heterogeneity of the surface, rather than features arising from decreased dipole–dipole coupling or direct repulsion upon desorption of the adsorbate are put into evidence [44]. The remaining catalyst samples displayed similar behavior

After the evacuated cell was cooled down to RT, a new dosis of 10 Torr CO(g) was admitted into it and a final IR spectrum was immediately recorded (hereafter labelled as

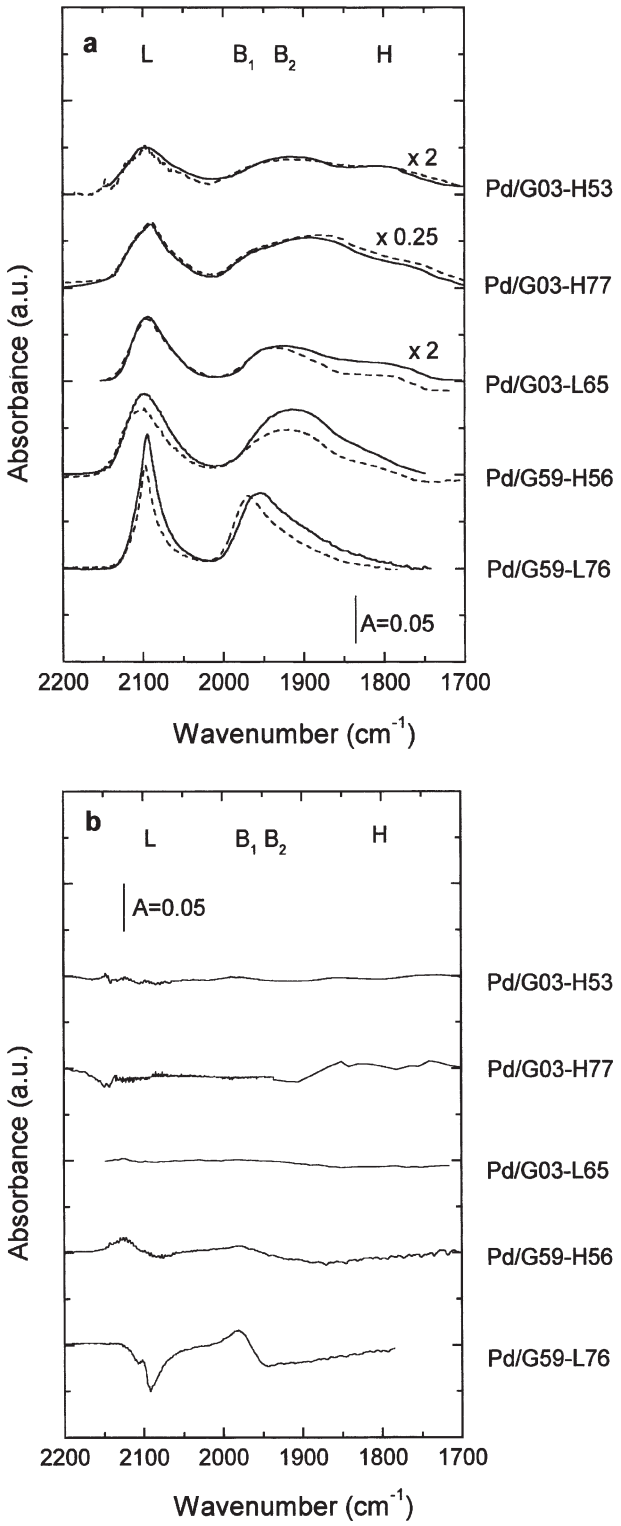

Figure 9. (a) Comparative spectra of adsorbed CO (10 Torr; 298 K) on the Pd/SiO_2 catalysts: continuous lines, initial exposure ($t^{I} = 0$ h); dashed lines, re-exposure ($t^{II} = 0$ h) after temperature-programmed desorption and cooling back to RT under vacuum. (b) Difference spectra ($t^{I} = 0$ h subtracted from the $t^{II} = 0$ h spectra).

$t^{II} = 0$ h). These spectra, together with the ones taken at $t^{I} = 0$ h in the first "cycle" are shown in figure 9(a), while their difference is presented in figure 9(b).

The comparison of both spectra shows that, with the only exception of the highly dispersed Pd/G59-L76 catalysts, the restructuring of the supported Pd crystallites after CO chemisorption at room temperature (with further TPD *in vacuo*) is a reversible phenomenon. That is, within the bounds of our experimental error (<10%), reproducible CO_s spectra are obtained for meso- and microporous silicas with both high and low loadings of Pd after a full adsorption–desorption cycle.

In section 1 we mentioned that Hicks et al. had recently reported that cycles of CO exposure and reduction of Pd/Al_2O_3 at ambient pressure (<200 Torr) smoothened the crystallite surfaces into well-ordered facets, whereas cycles of oxidation and reduction roughened the surfaces [16]. These workers, though, *reduced* their catalyst samples with hydrogen at high temperature prior to exposing them to "cycles" of CO exposure, which might well have sintered the Pd particles. Hence, we think that our experimental evidence of surface roughening does not contradict Hicks et al.'s data, as no H_2 reduction between cycles of CO exposure was done here.

Presently, it is not entirely clear to us why it is that CO chemisorption on Pd/G59-L76 is not fully reversible. Incomplete CO desorption, accompanied by carbon deposition due to disproportionation at high temperature, rather than metal sintering or coalescence stands out as the most likely cause of this reduction in chemisorption capacity [45,46]. Nonetheless, disproportionation/decomposition of CO on unpromoted Pd/SiO_2 was found to be less than 6% of the total CO_s by Rieck and Bell [42] and, also, the Pd/G59-L76 catalyst was the one that showed the lowest methanation activity at 523 K (table 2).

Is it, then, that an (unconstricted) high mobilitity of palladium particles on the mesoroporous silica brings in some sintering (i.e., a reduced CO chemisorption in a second adsorption cycle), whereas on the microporous support, even for the highly dispersed catalyst preparation, Pd/G03-H77, the restriction in mobility brought about by the support texture grants reversibility in CO chemisorption? More experiments should be done and/or the use of combined techniques should be applied so as to be able to weigh or distinguish among these possibilities.

4. Conclusions

It has been found that well dispersed Pd, supported on microporous silica (Davison G03) exhibits chemisorbed CO in multicoordinated or "hollow" sites, originated in the morphology of the support, while these signals are not shown by preparations of the supported metal of comparable dispersity on mesoporous G59 grade. Terminal (L band) and di-coordinated CO_s (B band) appear in both types of catalyst types, as it has been extensively reported in the past. The high-loading preparations on the microporous support showed a higher proportion of Pd(111) planes than those of low Pd loading, which seems to contribute to the high

TOF_{CH_4} and high selectivity to methane in syn-gas activation of these catalysts, while the remaining ones show excellent capability for methanol production.

Our experimental results indicate that these finely dispersed Pd particles experience profound changes upon long-term exposure to carbon monoxide at ambient conditions, chemisorbing more CO with either concomitant roughening of the surface (Pd/G03 and Pd/G59-H56) or showing more open crystal planes (Pd/G59-H76). This phenomenon of surface restructuring seems to depend both on the initial exposed metal fraction (FE) of palladium, i.e., on Pd particle size, and the morphology of the support. The rate of surface restructuring, but not its extent, is a function of the superimposed CO(g) pressure.

Despite the various changes experienced by the catalyst surfaces after CO exposure, the essential differences of the infrared spectra of chemisorbed CO between the Pd/G59 and Pd/G03 catalyst types observed at time zero remain after 18 h exposure. The predominant abundance of B_2 and H bands in the CO/FTIR spectra of the latter catalysts, which is indicative of a prevailing presence of the Pd(111) plane, can give an account of their better efficiency for CH_4 production [2,3]. It is then understandable that, if the rate-determining step for the complete hydrogenation of CO to methane is the dissociation of the C–O bond, microporous silica makes a poor material for obtaining suitable supported Pd catalysts for methanol synthesis purposes.

Although the influence of high pressure and/or temperature over the surface morphology of palladium crystallites cannot be ignored, our CO/FTIR results are at least directionally consistent with the performance shown by these Pd/SiO_2 catalysts under process conditions.

Acknowledgement

Thanks are given to Universidad Nacional del Litoral, Consejo Nacional de Investigaciones Científicas y Técnicas (CONICET) and the Japan International Cooperation Agency (JICA) for their financial support.

References

[1] M.L. Poutsma, L.F. Elek, P.A. Ibarbia, A.P. Risch and J.A. Rabo, J. Catal. 52 (1978) 157.
[2] J.S. Rieck and A.T. Bell, J. Catal. 103 (1987) 46.
[3] J.M. Driessen, E.K. Poels, J.P. Hindermann and V. Ponec, J. Catal. 82 (1983) 26;
G.V.D. Lee and V. Ponec, Catal. Rev. Eng. Sci. 29 (1987) 183.
[4] F. Fajula, R.G. Anthony and J.H. Lunsford, J. Catal. 73 (1982) 237.
[5] L. Sheu, H. Knözinger and W.M.H. Sachtler, J. Am. Chem. Soc. 111 (1989) 8125.
[6] A.L. Bonivardi, D.L. Chiavassa and M.A. Baltanás, in: *New Frontiers in Catalysis*, Proc. 10th Int. Congr. on Catal., Budapest, Hungary, Vol. B, eds. L. Guzci et al. (Elsevier, Amsterdam, 1993) p. 801.
[7] R.F. Hicks and A.T. Bell, J. Catal. 90 (1984) 205, and references therein.
[8] F.M. Hoffmann, Surf. Sci. Rep. 3 (1983) 1.
[9] R.F. Hicks, Q.-J. Yen and A.T. Bell, J. Catal. 89 (1984) 498.
[10] Z. Knor, Surf. Sci. 169 (1986) L317.
[11] G.A. Somorjai, *Introduction to Surface Chemistry and Catalysis* (Wiley, New York, 1994).
[12] B. Lang, R.W. Joner and G.A. Somorjai, Surf. Sci. 30 (1972) 440.
[13] D.W. Blakely and G.A. Somorjai, Surf. Sci. 65 (1977) 419.
[14] G.A. Somorjai and M.A. van Hove, Prog. Surf. Sci. 30 (1989) 201.
[15] M. El-Yakhloufi and L. Gillet, Catal. Lett. 17 (1993) 11.
[16] R.F. Hicks, H. Qi, A. Kooh and L. Fischel, J. Catal. 124 (1990) 488.
[17] A.L. Bonivardi and M.A. Baltanás, J. Catal. 125 (1990) 243.
[18] A.L. Bonivardi and M.A. Baltanás, Thermochim. Acta 191 (1991) 63.
[19] A.L. Bonivardi and M.A. Baltanás, J. Catal. 138 (1992) 500.
[20] L.L. Sheu, Z. Karpinksi and W.M.H. Sachtler, J. Phys. Chem. 93 (1989) 4890.
[21] R.P. Eischens and W.A. Pliskin, Adv. Catal. 10 (1958) 1.
[22] L.R. Becerra, C.P. Slichter and J.H. Sinfelt, Phys. Rev. B 52 (1995) 11457.
[23] R. Van Hardeveld and F. Hartog, Adv. Catal. 22 (1972) 75.
[24] L.L. Sheu, H. Knözinger and W.M.H. Sachtler, J. Mol. Catal. 57 (1989) 61.
[25] A.L. Bonivardi, Tesis Doctoral, Universidad Nacional del Litoral (1991).
[26] G.F. Froment and K.B. Bischoff, *Chemical Reactor Analysis and Design* (Wiley, Singapore, 1990).
[27] R.B. Bird, W.E. Stewart and E.N. Lightfoot, *Fenómenos de Transporte* (Reverté, Spain, 1964).
[28] P. Chou and M.A. Vannice, J. Catal. 104 (1987) 17.
[29] D.D. Eley and P.B. Moore, Surf. Sci. 111 (1981) 325.
[30] R. Greenler, K. Burch, K. Kretzschmar, R. Klauser, A.M. Bradshaw and B.E. Hayden, Surf. Sci. 152/153 (1985) 338.
[31] A.M. Bradshaw and F.M. Hoffmann, Surf. Sci. 72 (1978) 513.
[32] T.E. Madey, J.T. Yates, Jr., A.M. Bradshaw and F.M. Hoffmann, Surf. Sci. 89 (1979) 370.
[33] Y. Shen, L. Cai, J. Li, S. Wang and K. Huang, Catal. Today 6 (1989) 46.
[34] Y. Shen, J. Li, L. Cai and K. Huang, J. Mol. Catal. 59 (1990) 61.
[35] Y. Shen and K. Huang, Appl. Surf. Sci. 59 (1992) 187.
[36] H. Deligianni, R.L. Mieville and J.B. Peri, J. Catal. 95 (1985) 465.
[37] D.R. Lide, ed., *CRC Handbook of Chemistry and Physics*, 72nd Ed. (CRC Press, Boca Raton, 1991–1992).
[38] M.A. Vannice, J. Catal. 37 (1975) 462.
[39] R.J. Levis, J. Zhicheng and N. Winograd, J. Am. Chem. Soc. 111 (1989) 4605.
[40] F. Solymosi, A. Berkó and Z. Tóth, Surf. Sci. 285 (1993) 197.
[41] G. Bergeret, P. Gallezot and B. Imelik, J. Phys. Chem. 85 (1981) 411.
[42] J.S. Rieck and A.T. Bell, J. Catal. 96 (1985) 88.
[43] H. Conrad, G. Ertl, J. Koch and E.E. Latta, Surf. Sci. 43 (1974) 462.
[44] D.O. Hayward and B.M.W. Trapnell, *Chemisorption* (Butterworths, London, 1964).
[45] S. Ichikawa, H. Poppa and M. Boudart, J. Catal. 91 (1985) 1.
[46] V. Matolin, M. Rebholz and N. Kruse, Surf. Sci. 245 (1991) 233.